NASA TECHNICAL NOTE

NASA TN D-1948

NASA TN D-1948

APPLICATION OF TRANSTABILITY CONCEPT TO FLUTTER OF FINITE PANELS AND EXPERIMENTAL RESULTS

by Sidney C. Dixon;
Langley Research Center,
Langley Station, Hampton, Va.

NATIONAL AERONAUTICS AND SPACE ADMINISTRATION • WASHINGTON, D. C. • SEPTEMBER 1963

ERRATA

NASA Technical Note D-1948

APPLICATION OF TRANSTABILITY CONCEPT TO FLUTTER OF FINITE PANELS AND EXPERIMENTAL RESULTS

By Sidney C. Dixon
September 1963

Page 4, line 16, and page 28, line 4:

In the equation for ψ the expression $\left(\frac{a}{b}\right)^4$ appearing in the last term should be $\left(\frac{a}{h}\right)^4$. The correct equation is therefore

$$\psi = \pm \frac{12(1 + \mu)}{\pi^2} \left\{ \pm\alpha \, \Delta T \left(\frac{a}{h}\right)^2 - 0.25 \left[\frac{\Delta p}{E} \left(\frac{a}{h}\right)^4 \right]^{2/3} \right\}$$

NASA-Langley, 1964

Issued 12-18-64

TECHNICAL NOTE D-1948

APPLICATION OF TRANSTABILITY CONCEPT TO FLUTTER OF FINITE PANELS AND EXPERIMENTAL RESULTS

By Sidney C. Dixon

Langley Research Center
Langley Station, Hampton, Va.

NATIONAL AERONAUTICS AND SPACE ADMINISTRATION

NATIONAL AERONAUTICS AND SPACE ADMINISTRATION

TECHNICAL NOTE D-1948

APPLICATION OF TRANSTABILITY CONCEPT TO FLUTTER OF FINITE PANELS AND EXPERIMENTAL RESULTS*

By Sidney C. Dixon

SUMMARY

The flutter characteristics of finite panels are investigated both theoretically and experimentally. The theoretical analysis is based on the transtability concept which postulates that the loss of stable static equilibrium of a buckled panel results in dynamic instability or flutter. The differential equation, based on small-deflection theory and two-dimensional static aerodynamics, governing the buckling characteristics of panels subjected to supersonic airflow is solved by the Galerkin method. Numerical results for transtability flutter are obtained from four-term solutions for both simply supported and clamped panels with various length-width ratios and various ratios of lateral to longitudinal midplane compressive stress. The results indicate that for given boundary conditions there are many combinations of length-width ratio and stress ratio for which the thickness required to prevent flutter of a panel on the verge of buckling becomes very large.

In addition, experimental results are presented for essentially clamped panels with a length-width ratio of 4. The panels were tested at a Mach number of 3.0, at dynamic pressures ranging from 1,600 to 5,000 lb/sq ft, and at stagnation temperatures from 300° to 650° F. A boundary faired through the experimental flutter points consisted of a flat-panel portion, a buckled-panel portion, and a transition point, at the intersection of the two boundaries (onset of buckling), where a panel is most susceptible to flutter.

The experimental results for flutter at the onset of buckling were within the flutter region indicated by the small-deflection transtability calculations. Both theory and experiment indicate that existing experimental flutter envelopes can be inadequate as flutter criteria for stressed panels.

---

*Most of the information presented herein was submitted to the University of Virginia in partial fulfillment of the requirements for a Master of Applied Mechanics degree under the title "Investigation of Flutter Characteristics of Rectangular Panels on the Verge of Buckling," April 1963.

INTRODUCTION

The susceptibility to flutter of the outer skins of components of several current aircraft (see ref. 1) has resulted in the emergence of panel flutter as a significant factor in the design of supersonic and hypersonic vehicles. Although the phenomenon of panel flutter has been the subject of numerous investigations (see the comprehensive summary paper by Fung, ref. 2), generally poor agreement between theory and experiment exists for other than the simplest configuration of low length-width ratio. Thus, to a large extent, existing panel-flutter criteria are based on the most conservative experimental data available, such as the flutter envelopes presented in references 3 and 4. For panels that have large length-width ratios and are subjected to in-plane loading, large differences between theory and experiment have been shown in both the flutter boundaries and flutter modes. (See, for example, ref. 5.) For such panels, the buckling characteristics appear to have considerable influence on the flutter boundaries and, in fact, experimental results indicate that the most critical flutter condition occurs in the vicinity of the panel buckling load. (See, for example, refs. 6, 7, and 8.)

In the present investigation the flutter characteristics of finite rectangular panels subjected to compressive loads near the critical buckling load are examined theoretically by means of the transtability concept introduced by Isaacs (ref. 9). The term transtability refers to the loss of stable static equilibrium of a buckled panel when the speed of flow exceeds a certain critical value (transtability value). The relations between results obtained from the static transtability analysis (based on small-deflection theory) and the large-deflection dynamic analysis of Fralich (ref. 10) are reviewed and are compared qualitatively with experimental trends. Modal solutions of the governing differential equation (based on two-dimensional static aerodynamics) for thin isotropic plates (ref. 11) are obtained by the Galerkin method. Numerical results for both simply supported and clamped-edge panels with length-width ratios up to 4 are presented for various ratios of lateral to longitudinal midplane compressive stress.

In addition, experimental results obtained from tests of essentially clamped panels with a length-width ratio of 4 are presented. Single-bay panels, 25 inches long and 6.25 inches wide, were tested in the Langley 9- by 6-foot thermal structures tunnel at a Mach number of 3.0 at various dynamic pressures and stagnation temperatures. The experimental data are presented in tabular form and are also summarized in terms of nondimensional parameters in the form of a flutter boundary. Theoretical and experimental results are compared for the flutter of panels subjected to compressive loads near the critical buckling load.

SYMBOLS

$$\overline{A}_C = \overline{R}_X - 2.49\left(\frac{a}{b}\right)^2$$

$$\overline{A}_S = \overline{R}_X - 2\left(\frac{a}{b}\right)^2$$

a panel length (longitudinal direction, parallel to airflow)

a_n modal amplitude coefficient

$$\bar{B}_c = 1.25\bar{R}_y\left(\frac{a}{b}\right)^2 - 5.14\left(\frac{a}{b}\right)^4$$

$$\bar{B}_s = \bar{R}_y\left(\frac{a}{b}\right)^2 - \left(\frac{a}{b}\right)^4$$

b panel width (lateral direction, perpendicular to airflow)

D panel stiffness, $\dfrac{Eh^3}{12\left(1 - \mu^2\right)}$

E Young's modulus

f flutter frequency

h thickness of panel skin

M Mach number

m,n integers

$N_x = \sigma_x h$

$N_y = \sigma_y h$

p_∞ free-stream static pressure

p_b static pressure in cavity behind panel

Δp differential pressure acting on panel skin, $p_b - p_\infty$

q free-stream dynamic pressure

$$\bar{R}_x = \frac{N_x a^2}{\pi^2 D}$$

$$\bar{R}_y = \frac{N_y a^2}{\pi^2 D}$$

T temperature

T_t stagnation temperature

ΔT increase of panel skin temperature (averaged along center line)

t time

w vertical deflection of panel

$$\overline{w}(\xi) = \sum_{n=1}^{N} a_n \phi_n(\xi)$$

x,y,z cartesian coordinates (fig. 2)

α coefficient of thermal expansion of panel skin

$$\beta = \sqrt{M^2 - 1}$$

$$\xi = \frac{x}{a}$$

$\theta(y)$ first normal mode of vibration of uniform clamped-clamped beam

λ dynamic-pressure parameter, $\frac{2qa^3}{\beta D}$

μ Poisson's ratio (taken equal to 0.3)

σ_x midplane stress in x-direction (positive in compression)

σ_y midplane stress in y-direction (positive in compression)

$\phi_n(\xi)$ nth normal mode of vibration of uniform clamped-clamped beam

$$\psi = \pm \frac{12(1 + \mu)}{\pi^2} \left\{ \pm\alpha \Delta T \left(\frac{a}{h}\right)^2 - 0.25 \left[\frac{\Delta p}{E} \left(\frac{a}{b}\right)^4 \right]^{2/3} \right\}$$

Subscript:

T transtability

THEORY

The flutter of buckled panels has been the subject of numerous investigations (see comprehensive summary paper by Fung, ref. 2). Isaacs (ref. 9) first considered the flutter of buckled panels on the basis of small-deflection theory and introduced the concept of transtability flutter of two-dimensional panels. This concept is based on purely static considerations of the buckling characteristics of a panel when exposed to supersonic flow. The term transtability refers to the loss of stable static equilibrium of the buckled panel when the speed of flow exceeds a certain critical value, that is, the transtability value. The results of large-deflection dynamic analyses (see, for example, refs. 12 and 13) have revealed that the transtability speed is essentially the flutter speed of two-dimensional panels for small perturbations about the static, buckled, equilibrium position.

Hedgepeth (ref. 14) used the transtability concept, in conjunction with small-deflection theory and two-dimensional static aerodynamics, in a two-mode analysis of rectangular simply supported panels. Hedgepeth argued that the results of such an analysis correctly represent the limiting case of vanishingly small buckle depths and that this limiting case establishes a lower bound on the critical value of the dynamic-pressure parameter λ for flutter of buckled panels. Leonard and Hedgepeth (ref. 11) used the transtability concept in a similar analysis of rectangular clamped panels. Their results were in fair agreement with experimental data for panels with length-width ratios of about 2 or less.

Hedgepeth's conjecture that the transtability concept (and small-deflection theory) may be applied to finite panels appears to be justified by the results of a recent large-deflection dynamic analysis by Fralich (ref. 10). Fralich investigated the flutter characteristics of finite simply supported panels in both the prebuckling and postbuckling conditions and utilized two-dimensional static aerodynamics. Figure 1 shows typical results obtained by Fralich in terms of the dynamic-pressure parameter λ and the edge-load parameter $\bar{R}_x$. The results shown are for a panel with length-width ratio a/b of 1 subjected to loading such that the stress ratio $\frac{N_y}{N_x} = 1$. The solid curve is the flutter boundary above which the panel is dynamically unstable; below the boundary the panel is dynamically stable and is either flat or buckled. (A thorough discussion of the various stability regions is given in ref. (10)). As can be seen from figure 1, an increase in $\bar{R}_x$ results in a decrease in λ if the panel is flat when dynamically stable but results in an increase in λ if the panel is buckled. Thus the minimum value of λ required for flutter occurs at the intersection of the flat-panel and buckled-panel boundaries. The trends exhibited by the overall flutter boundary are in qualitative agreement with experimental results for heated panels. (See, for example, refs. 6, 7, and 8.) The intersection of the flat-panel and buckled-panel boundaries, where a panel is most susceptible to flutter, has been referred to by some experimental investigators as the transition point (see, for example, ref. 8) and in this investigation is considered to be the flutter point for a panel on the verge of buckling.

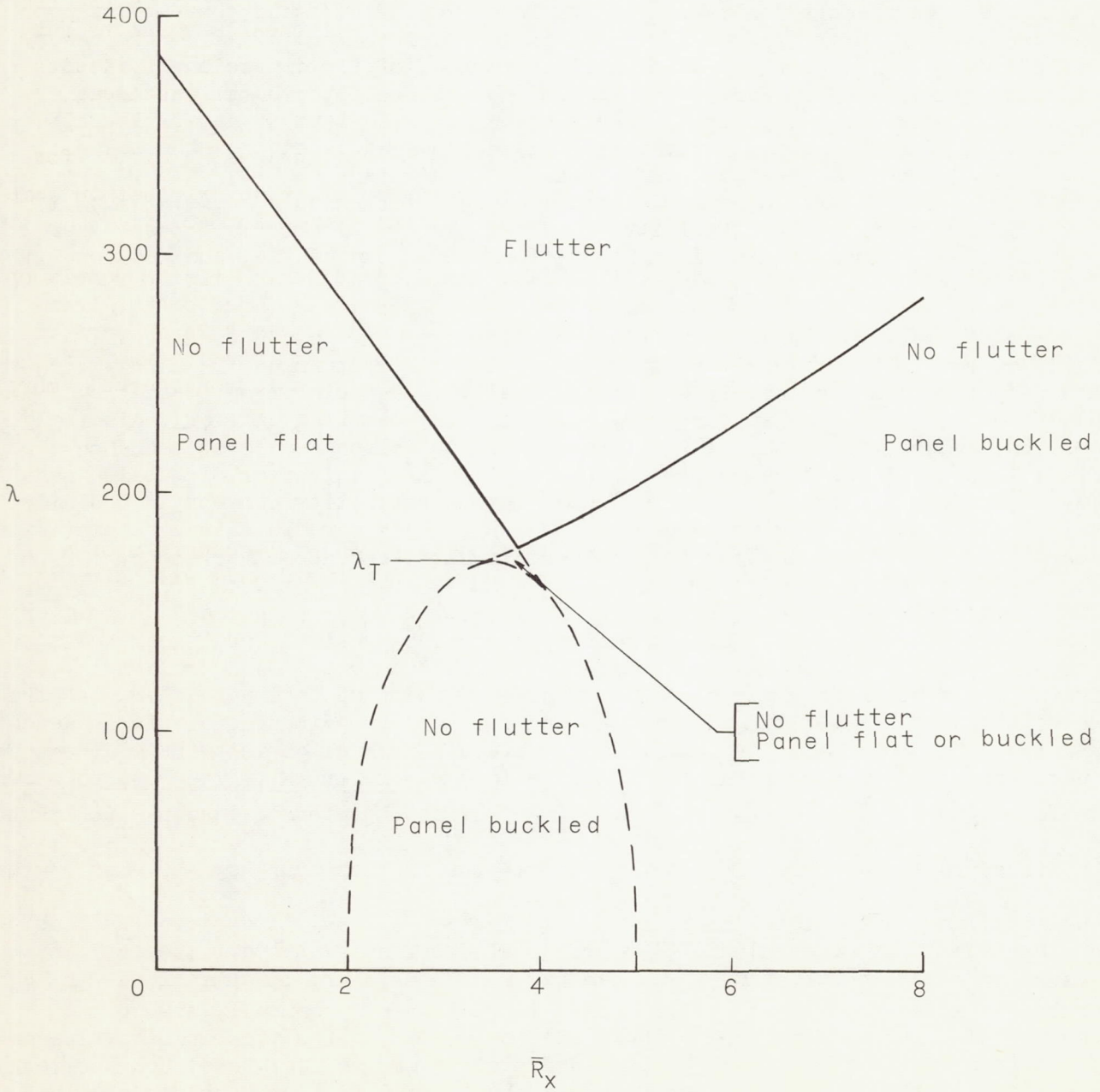

Figure 1.- Effects of compressive stress and buckling on flutter of simply supported panel as obtained by Fralich (ref. 10). $\frac{a}{b} = 1$; $\frac{N_y}{N_x} = 1$.

The dashed loop shown in figure 1 gives the variation of the critical values of $\bar{R}_x$ for buckling with airflow. On the basis of small-deflection theory the peak of the buckling loop represents the value of λ above which no stable, static, buckled equilibrium position exists. Thus, this value of λ is the transtability value λ_T. As can be seen from figure 1, λ_T is nearly equal to but slightly less than the value of λ at the transition point. Fralich's results for other specified values of a/b and N_y/N_x indicated, in some instances, that the overall flutter trends could be different from those shown in figure 1 but that λ_T was always equal or nearly equal to the critical value of λ for flutter at the transition point. It should be pointed out, however, that in some instances λ_T was larger than the value of λ at the transition point.

In the present investigation the flutter characteristics of finite panels on the verge of buckling are again considered. The analysis is based on the transtability concept since the error introduced by this static analysis appears to be small and since the procedure required to obtain numerical results from the more refined, and complex, large-deflection dynamic analysis is considerably more laborious.

Analysis

The configuration to be analyzed is shown in figure 2. It consists of a rectangular panel of uniform thickness h mounted in a rigid wall with air

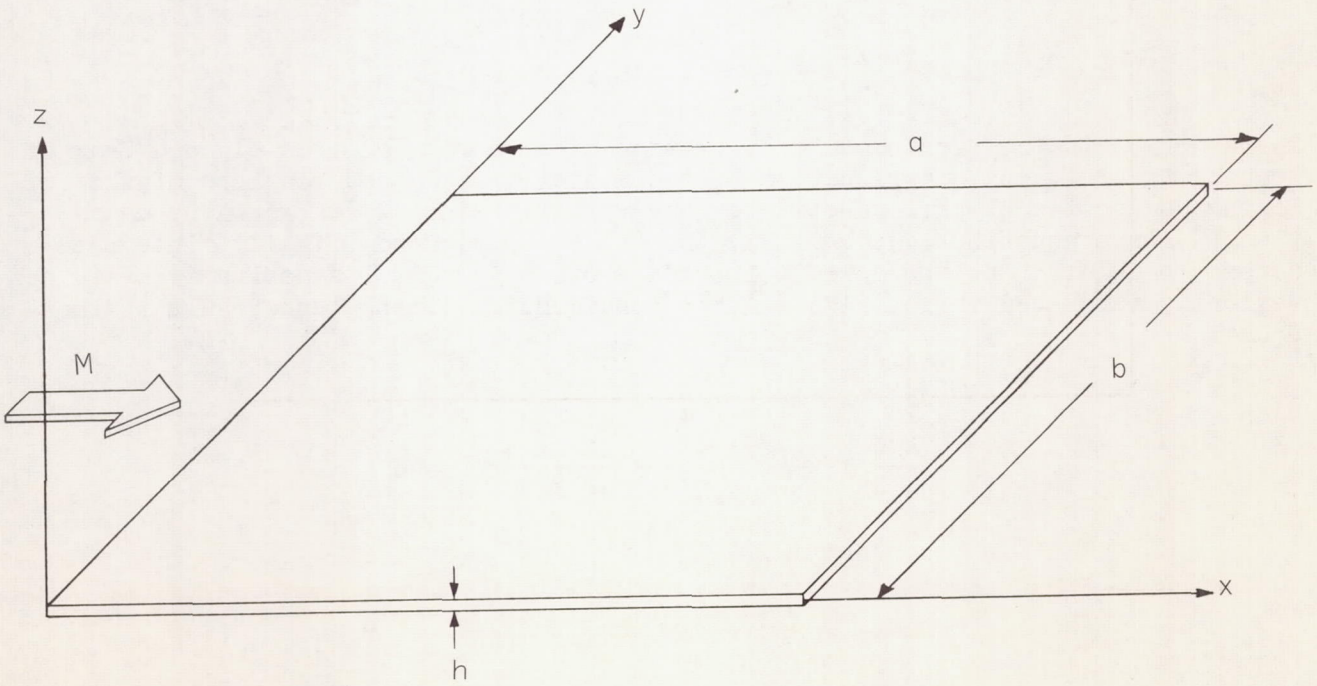

Figure 2.- Rectangular panel and coordinate system.

flowing over one surface at a Mach number M. The plate has a length a and width b and is subjected to uniform midplane compressive forces N_x and N_y. If the aerodynamic loading is represented by the air forces yielded by linearized static aerodynamic strip theory, the governing partial differential equation is (from ref. 11)

$$D\left(\frac{\partial^4 w}{\partial x^4} + 2\frac{\partial^4 w}{\partial x^2 \partial y^2} + \frac{\partial^4 w}{\partial y^4}\right) + N_x \frac{\partial^2 w}{\partial x^2} + N_y \frac{\partial^2 w}{\partial y^2} + \frac{2q}{\beta}\frac{\partial w}{\partial x} = 0 \tag{1}$$

Clamped panels.- The appropriate boundary conditions for a panel with all edges clamped are

$$\left.\begin{aligned} w(x,0) = w(x,b) = w(0,y) = w(a,y) = 0 \\ \frac{\partial w}{\partial y}(x,0) = \frac{\partial w}{\partial y}(x,b) = \frac{\partial w}{\partial x}(0,y) = \frac{\partial w}{\partial x}(a,y) = 0 \end{aligned}\right\} \tag{2}$$

Equation (1) may be reduced to an ordinary differential equation approximately representing the clamped panel (by the Kantorovich method, ref. 15) if the deflection shape in the y-direction is assumed to be given by a single function satisfying the prescribed boundary conditions. Let

$$w = \overline{w}(x)\theta(y) \tag{3}$$

where $\theta(y)$ is the first mode of vibration of a uniform clamped-clamped beam of length b (ref. 16). Application of the Kantorovich method consists of the following successive steps: substitute the expression for w as given by equation (3) into equation (1); multiply through by $\theta(y)$; and, finally, integrate across the width (the appropriate integrals of $\theta(y)$ and its derivatives are conveniently tabulated in ref. 17). After nondimensionalizing, the result is the equation

$$\frac{d^4\overline{w}}{d\xi^4} + \pi^2\overline{A}_c\frac{d^2\overline{w}}{d\xi^2} + \lambda\frac{d\overline{w}}{d\xi} - \pi^4\overline{B}_c\overline{w} = 0 \tag{4}$$

where

$$\left.\begin{aligned} \xi &= \frac{x}{a} \\ \bar{A}_c &= \frac{N_x a^2}{\pi^2 D} - 2.49\left(\frac{a}{b}\right)^2 = \bar{R}_x - 2.49\left(\frac{a}{b}\right)^2 \\ \lambda &= \frac{2qa^3}{\beta D} \\ \bar{B}_c &= 1.25\,\frac{N_y a^2}{\pi^2 D}\left(\frac{a}{b}\right)^2 - 5.14\left(\frac{a}{b}\right)^4 = 1.25\bar{R}_y\left(\frac{a}{b}\right)^2 - 5.14\left(\frac{a}{b}\right)^4 \end{aligned}\right\} \tag{5}$$

Substitution of the well-known exact solution of equation (4) into the appropriate boundary conditions results in the stability equation (see ref. 18)

$$4\delta\eta(\cosh 2\epsilon - \cosh\delta\cos\eta) + 2\left(\delta^2 - \eta^2 - 4\epsilon^2\right)\sinh\delta\sin\eta = 0 \tag{6}$$

where

$$\left.\begin{aligned} \delta^2 &= \frac{\lambda}{4\epsilon^2} - \left(\epsilon^2 + \frac{\pi^2\bar{A}_c}{2}\right) \\ \eta^2 &= \frac{\lambda}{4\epsilon^2} + \left(\epsilon^2 + \frac{\pi^2\bar{A}_c}{2}\right) \end{aligned}\right\} \tag{7}$$

and thus

$$\bar{B}_c = \frac{1}{\pi^4}\left[\frac{\lambda^2}{16\epsilon^2} - \left(2\epsilon^2 + \frac{\pi^2\bar{A}_c}{2}\right)^2\right] \tag{8}$$

Solutions in terms of the parameters $\bar{A}_c$, λ, and $\bar{B}_c$ are readily obtained when λ and either $\bar{A}_c$ or $\bar{B}_c$ are specified and the remaining parameter is treated as the eigenvalue. However, to study the flutter characteristics of panels on the verge of buckling, it is desirable to specify the panel length-width

ratio a/b and stress ratio N_y/N_x. Once these ratios are specified, $\bar{A}_c$ and $\bar{B}_c$ are functions only of $\bar{R}_x$ $\left(\text{since } \bar{R}_y = \frac{N_y}{N_x}\bar{R}_x\right)$ and thus $\bar{R}_x$ may then be treated as the eigenvalue. For this case considerable labor is required to obtain results from equation (6). Thus it is desirable to solve equation (4) by the Galerkin method. However, numerical results were obtained from equation (6) to determine the variation of $\bar{B}_c$ with $\bar{A}_c$ for no airflow ($\lambda = 0$) for comparison with the approximate results obtained from the Galerkin solution.

Equation (4) may be solved approximately by the Galerkin method as follows. Let

$$\bar{w} = \sum_{n=1}^{N} a_n \phi_n(\xi) \tag{9}$$

where the expansion function $\phi_n(\xi)$ is the nth mode of vibration of a uniform clamped-clamped beam of unit length. Substituting into equation (4), multiplying by $\phi_m(\xi)$, and integrating yields a set of N simultaneous equations for the coefficients a_n. For a nontrivial solution, the determinant of the coefficients of a_n must equal zero. For $N = 4$ the result is

$$\begin{vmatrix} (500.56 - 121.42\bar{A}_c - 97.41\bar{B}_c) & -3.34\lambda & 96.17\bar{A}_c & -0.91\lambda \\ 3.34\lambda & (3{,}803.14 - 454.50\bar{A}_c - 97.41\bar{B}_c) & -5.52\lambda & 169.21\bar{A}_c \\ 96.17\bar{A}_c & 5.52\lambda & (14{,}619.72 - 976.08\bar{A}_c - 97.41\bar{B}_c) & -7.63\lambda \\ 0.91\lambda & 169.21\bar{A}_c & 7.63\lambda & (39{,}941.93 - 1{,}693.43\bar{A}_c - 97.41\bar{B}_c) \end{vmatrix} = 0 \tag{10}$$

The effects of the air forces λ on the buckling load $\bar{R}_x$ can be obtained from equation (10) for specified values of the length-width ratio a/b and stress ratio N_y/N_x. These results can then be examined to determine the largest value of λ for which a stable, static, buckled equilibrium position exists. This value of λ is the transtability value λ_T; in this investigation λ_T is considered to be the critical value required for flutter of a panel on the verge of buckling.

Simply supported panels.- The general expression for the simultaneous equations resulting from a Galerkin solution of equation (1) for all edges simply supported is presented in reference 14. For the sake of completeness, the determinant obtained for

$$w = \sin \frac{\pi y}{b} \sum_{n=1}^{4} \sin \frac{n\pi x}{a}$$

is presented herein:

$$\begin{vmatrix} 1 - \bar{A}_S - \bar{B}_S & -2.67 \frac{\lambda}{\pi^4} & 0 & -1.07 \frac{\lambda}{\pi^4} \\ 2.67 \frac{\lambda}{\pi^4} & 16 - 4\bar{A}_S - \bar{B}_S & -4.80 \frac{\lambda}{\pi^4} & 0 \\ 0 & 4.80 \frac{\lambda}{\pi^4} & 81 - 9\bar{A}_S - \bar{B}_S & -6.85 \frac{\lambda}{\pi^4} \\ 1.07 \frac{\lambda}{\pi^4} & 0 & 6.85 \frac{\lambda}{\pi^4} & 256 - 16\bar{A}_S - \bar{B}_S \end{vmatrix} = 0 \qquad (11)$$

where

$$\left.\begin{aligned} \bar{A}_S &= \bar{R}_X - 2\left(\frac{a}{b}\right)^2 \\ \bar{B}_S &= \bar{R}_Y\left(\frac{a}{b}\right)^2 - \left(\frac{a}{b}\right)^4 \end{aligned}\right\} \qquad (12)$$

Results and Discussion

Transtability flutter speeds can be determined from equation (10) for panels with all edges clamped and from equation (11) for all edges simply supported. The flutter characteristics of panels on the verge of buckling depend, to a large extent, on the panel length-width ratio a/b, the stress ratio N_y/N_x, and the panel boundary conditions. However, before considering the effects of these parameters, it would be advantageous to consider the panel buckling characteristics in the absence of airflow ($\lambda = 0$).

Panel buckling characteristics for no airflow.- The exact buckling characteristics of simply supported panels (for the modes considered) with no airflow may be obtained from equation (11) since the exact modes $\left(\sin \frac{\pi y}{b} \sin \frac{n\pi x}{a}\right)$, which satisfy both the boundary conditions and the governing partial differential equation (eq. (1)), were used as the expansion functions in the analysis. Examination of equation (11) reveals that with no airflow there is no cross coupling of the expansion functions. Thus the determinant is satisfied if each diagonal term is independently zero; this results in a linear variation of $\overline{B}_S$ with $\overline{A}_S$. The exact solution of equation (1) for clamped panels is not known. In order to obtain an approximate solution the partial differential equation (eq. (1)) was reduced to an ordinary differential equation (eq. (4)) approximately representing a clamped panel by the Kantorovich method. Equation (4) was then solved by the Galerkin method to obtain the stability determinant (eq. (10)). To investigate the convergence of results obtained from equation (10), numerical results were obtained from equation (6) (the exact solution of eq. (4)) for no airflow. The numerical results obtained from equations (10) and (6) are presented in figure 3 in terms of $\overline{B}_C$ and $\overline{A}_C$. The dot-dashed lines represent results obtained from two-term solutions for two consecutive expansion functions (the pertinent determinants are contained in eq. (10)), the dashed curves represent four-term results, and the solid curves are the results obtained from equation (6).

As can be seen in figure 3, the two-term solutions give a linear variation of $\overline{B}_C$ with $\overline{A}_C$. Examination of equation (10) reveals that for a two-term solution $\overline{A}_C$ and $\overline{B}_C$ do not appear in the off-diagonal terms and thus there is no cross coupling of the expansion functions; therefore, setting the diagonal terms equal to zero gives the variation of $\overline{B}_C$ with $\overline{A}_C$. The buckling modes (which in this case are the expansion functions) associated with the resulting straight lines are readily identified and are indicated by the sketches in figure 3. In contrast to the two-term results, however, equation (6) and the four-term solution do not give a linear variation of $\overline{B}_C$ with $\overline{A}_C$ for clamped panels. Equation (10) shows that when four terms are used, coupling occurs between the first and third expansion functions and the second and fourth expansion functions and thus the variation of $\overline{B}_C$ with $\overline{A}_C$ becomes nonlinear. The identification of the modes obtained from the exact and four-term solutions for a given value of $\overline{A}_C$ was based on the trends obtained from the two-term results. For example, the curve obtained from the exact solution which gives a value of $\overline{B}_C = 50$ for $\overline{A}_C = 10$ (fig. 3) is assumed to be associated with a mode shape having three half-waves in the x-direction; at $\overline{A}_C = 30$ this same curve is assumed to be associated with a shape having only one half-wave in the x-direction.

Figure 3 gives the buckling characteristics of clamped panels for no airflow in terms of the nondimensional parameters $\overline{B}_C$ and $\overline{A}_C$. If the panel length-width ratio a/b and stress ratio N_y/N_x are specified, the value of $\overline{R}_X$ for buckling can be determined from figure 3. For example, figure 4 shows the value of $\overline{R}_X$ required for buckling (with no airflow) as a function of a/b for $\frac{N_y}{N_x} = 1$. These

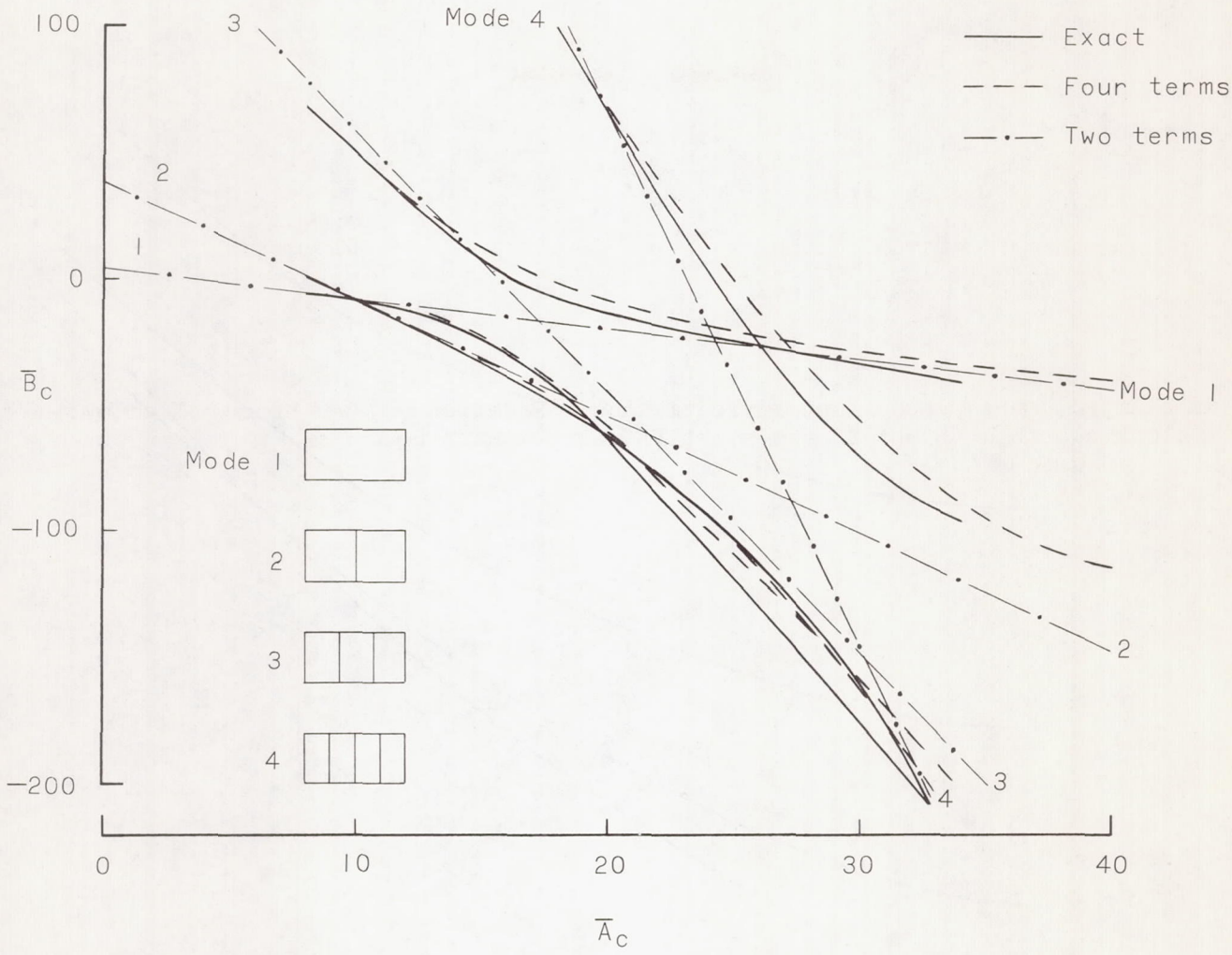

Figure 3.- Variation of $\overline{B}_c$ with $\overline{A}_c$ for no airflow. All edges clamped.

results were obtained from the four-term results shown in figure 3. Note that mode 1 is not necessarily the critical buckling mode.

Referring again to figure 3, it is seen that the four-term results are in good numerical agreement with the results obtained from equation (6) for small values of $\overline{A}_c$ $\left(\overline{A}_c < 10\right)$ where the buckling mode has one half-wave in the x-direction. For larger values of $\overline{A}_c$ $\left(\overline{A}_c > 20\right)$, where the buckling mode has two or more half-waves in the x-direction, the agreement is only fair; additional terms must be used to obtain good agreement in this region. However, the results suggest that the four-term analysis should be adequate for predicting trends even though the numerical results are only approximate. It is interesting to note that the two-term results are in fair to good agreement with the results obtained from equation (6) except in the vicinity of the values of $\overline{A}_c$ for which the two-term

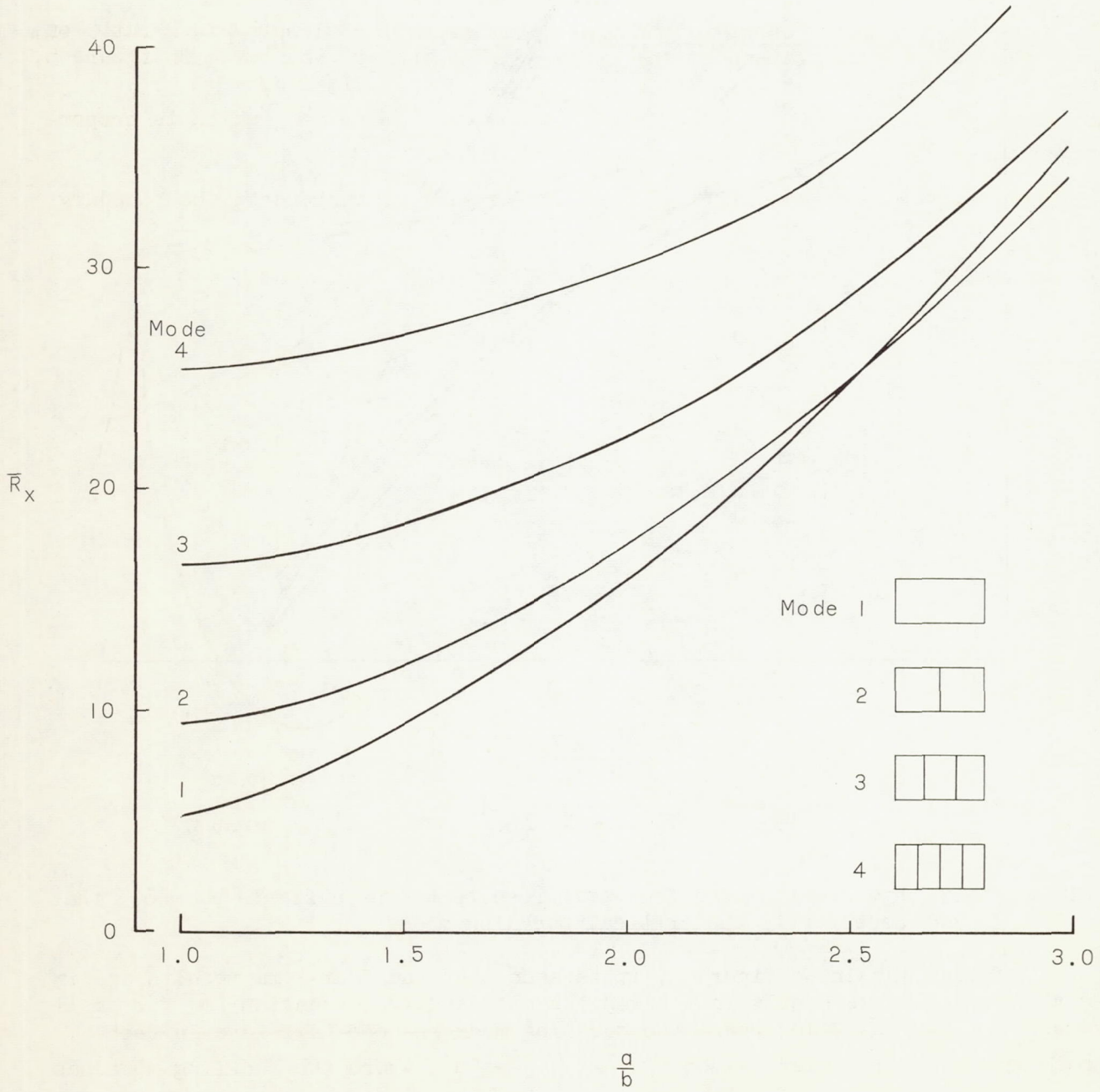

Figure 4.- Variation of buckling load and mode with panel length-width ratio for no airflow.

All edges clamped; $\frac{N_y}{N_x} = 1.0$.

solutions indicate that the values of $\overline{B}_c$ associated with modes 1 and 3 $\left(\overline{A}_c = 17, \text{ fig. } 3\right)$ and modes 2 and 4 $\left(\overline{A}_c = 27\right)$ are equal.

Effects of panel length-width ratio.- Some effects of length-width ratio on the flutter of clamped panels on the verge of buckling are indicated in figure 5, which shows the variation of the flutter parameter $\left(\frac{\beta E}{q}\right)^{1/3} \frac{h}{a}$ $\left(\text{which is proportional to } \frac{1}{\lambda^{1/3}}\right)$ with a/b for $\frac{N_y}{N_x} = 1.0$. The pair of numbers on the boundary

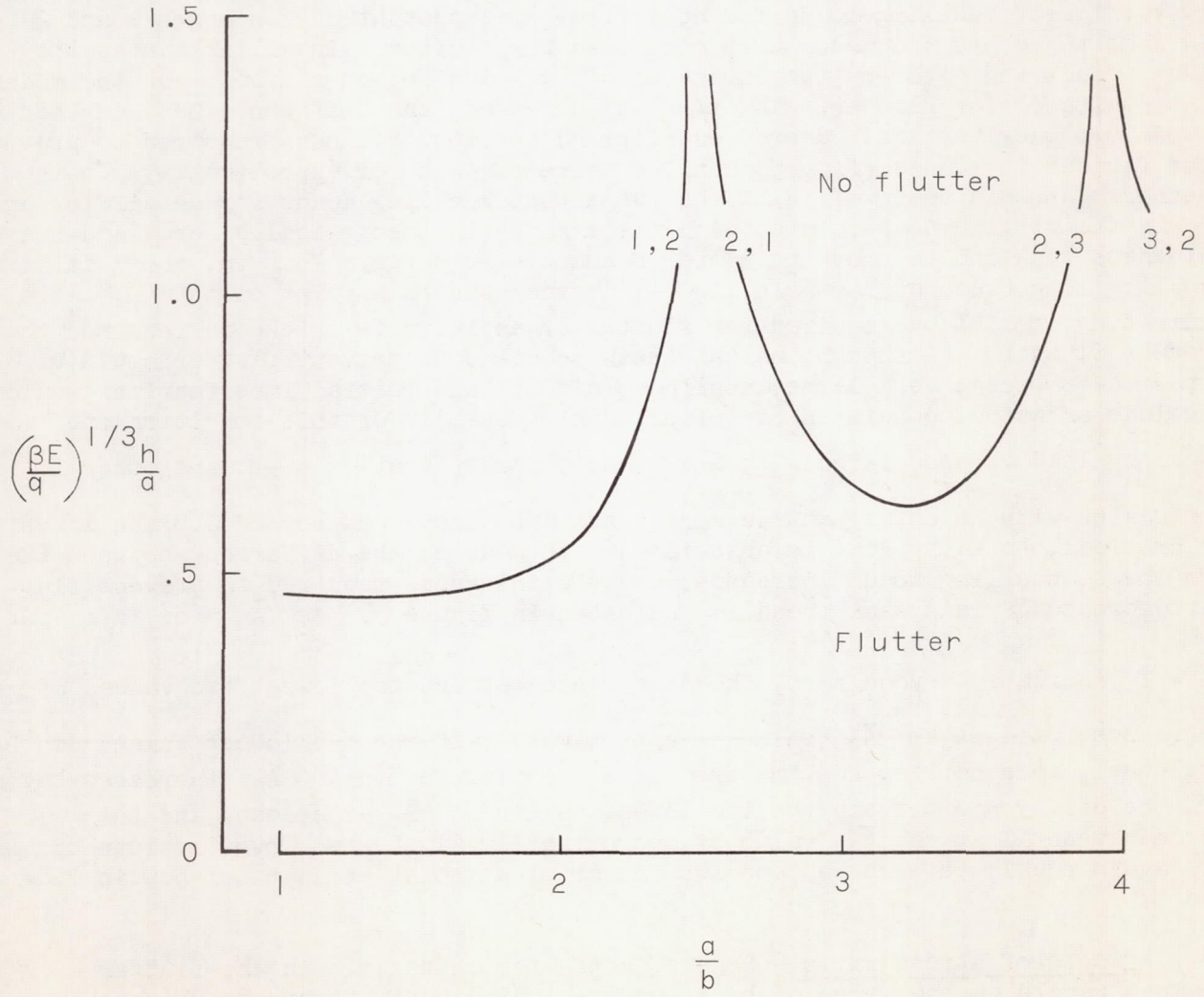

Figure 5.- Flutter characteristics of clamped panels on the verge of buckling for $\frac{N_y}{N_x} = 1.0$. The numbers on the boundaries indicate the modes that coalesced for flutter.

indicate the buckling modes that coalesced (at the peak of the buckling loop) for flutter. The first number indicates the number of half-waves in the x-direction of the mode associated with the lowest, or critical, buckling load for no airflow; the second number applies to the mode associated with the next lowest buckling load. As can be seen from figure 5, the thickness required to prevent flutter for $\frac{N_y}{N_x} = 1$ becomes very large for certain critical values of a/b (approximately 2.5 and 3.9).

The reason for the existence of such a flutter boundary can be more readily explained in conjunction with the panel buckling characteristics for no airflow shown in figure 4. Referring to figures 4 and 5, it is seen that for $\frac{a}{b} = 1.0$ the two lowest buckling loads for no airflow are associated with modes 1 and 2 and that these are the modes that coalesced for flutter. In all instances the modes associated with the two lowest buckling loads for no airflow were the modes that coalesced for flutter. As a/b is increased, the difference between the lowest two buckling loads decreases (fig. 4) and the thickness required to prevent flutter increases (fig. 5) until a value of a/b of approximately 2.5 is reached. At this value of a/b the two lowest buckling loads for no airflow are equal, the stiffness associated with these modes is theoretically zero, and the thickness required to prevent flutter becomes very large. That is, the static buckling loop (such as shown in fig. 1) degenerates to a point on the $\overline{R}_x$ axis indicating no airflow required for flutter or an infinite thickness required to prevent flutter. (Although the thickness required to prevent flutter could be expected to become very large, nonlinear effects and initial imperfections would preclude an actual condition of infinite thickness.) For this condition one buckling load is associated with a symmetric mode $\left(\text{about } x = \frac{a}{2}\right)$, the other is associated with an antisymmetric mode. As a/b increases beyond 2.5 the lowest, or critical, buckling load is associated with mode 2; the difference between the two lowest buckling loads increases; and the thickness required to prevent flutter decreases. This same trend is indicated in figure 3. As $\overline{A}_c$ $\left(\text{or } a/b \text{ for } \frac{N_y}{N_x} = 1\right)$ increases beyond zero, the difference between the lowest two values of $\overline{B}_c$ decreases until at an $\overline{A}_c$ value of approximately 10 the two lowest values of $\overline{B}_c$ are equal; this corresponds to a/b of 2.5 in figure 5. As $\overline{A}_c$ increases beyond 10, the difference between the two lowest values of $\overline{B}_c$ increases and then decreases until at an $\overline{A}_c$ value of approximately 21 the two lowest values of $\overline{B}_c$ are again equal; this corresponds to the critical point at a/b of 3.9 in figure 5.

Effects of stress ratio.- Some effects of stress ratio on the flutter of clamped panels on the verge of buckling are indicated in figure 6, which shows the variation of $\left(\frac{\beta E}{q}\right)^{1/3} \frac{h}{a}$ with N_y/N_x for $\frac{a}{b} = 4.0$. The flutter trends obtained by varying N_y/N_x while a/b is held constant are similar to the trends

obtained by varying a/b while N_y/N_x is held constant. The results shown in figure 6 indicate that infinite thickness is required to prevent flutter when N_y/N_x is approximately 0.82 and 1.02; these critical points correspond to values of $\bar{A}_c$ of approximately 33 and 21, respectively (fig. 3).

These results and the results of the previous section substantiate the statement of Leonard and Hedgepeth (ref. 11) that the theoretical flutter behavior of panels on the verge of buckling is quite sensitive to the panel buckling characteristics. If numerical results were obtained for a greater range of a/b and

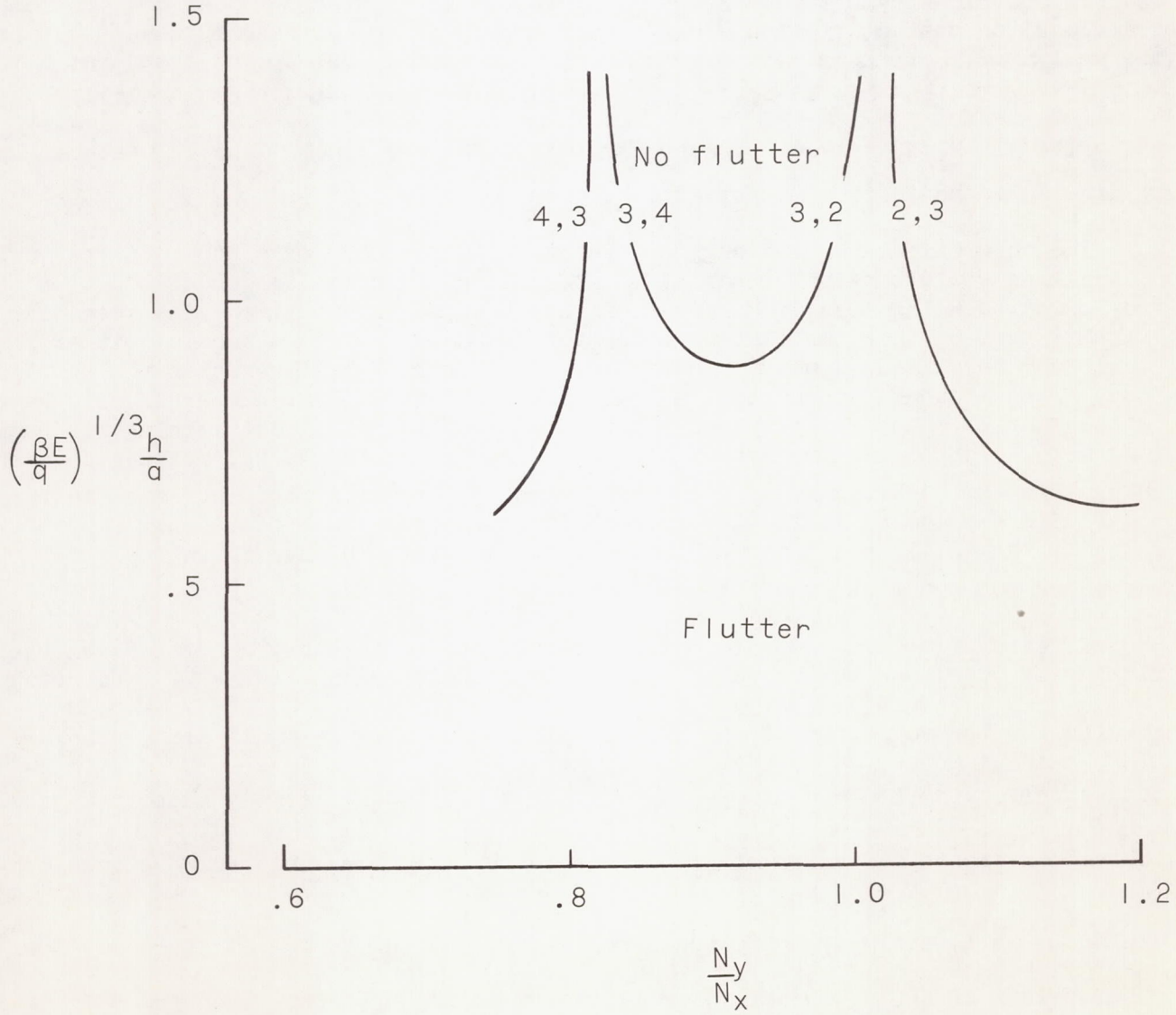

Figure 6.- Flutter characteristics of clamped panels on the verge of buckling for $\frac{a}{b} = 4.0$. The numbers on the boundaries indicate the modes that coalesced for flutter.

N_y/N_x (or $\bar{A}_c$), it would be found that there are many critical combinations of a/b and N_y/N_x for which the thickness required to prevent flutter approaches infinity. Although nonlinear effects would preclude a condition of infinite thickness to prevent flutter, it is apparent that these critical combinations of a/b and N_y/N_x should be avoided in design.

The critical combinations of a/b and N_y/N_x can be predicted for simply supported and clamped edges from existing buckling charts (for no airflow), such as those presented in reference 19, by determining the values of a/b and N_y/N_x for which the panel has an equal choice of buckling in two modes, one symmetric and the other antisymmetric. However, it should be pointed out that the theoretical buckling characteristics are strongly dependent on the assumed modes used in the analysis. For example, the results of reference 19 do not indicate that a clamped panel with $\frac{a}{b} = 4$ will buckle in the second mode and thus do not indicate the critical N_y/N_x values of approximately 1.02 (see fig. 6) and 1.3 (not shown in fig. 6) found in this investigation.

The theoretical results suggest that the flutter mode of a panel on the verge of buckling would consist primarily of a coupling of the modes associated with the two lowest buckling loads. Moreover, it has been shown experimentally (see, for example, ref. 6) that the flutter modes for thermally stressed panels (either buckled or unbuckled) appear to have the same number of half-waves as the buckling mode. Thus it would appear that a reasonable estimate of the number of half-waves in the flutter mode of a stressed panel could be obtained by determining its buckling mode. In this event, variations in the stress ratio N_y/N_x, which can cause changes in the buckling mode of a panel, might be expected to change the flutter mode. Since a change in flutter mode could be expected to affect other flutter characteristics, it would appear that the stress ratio N_y/N_x is an important parameter for the flutter of stressed panels.

Effects of boundary conditions.- Some effects of boundary conditions on the flutter of panels on the verge of buckling are indicated in figure 7. Numerical results for the variation of $\left(\frac{\beta E}{q}\right)^{1/3} \frac{h}{a}$ with a/b when $\frac{N_y}{N_x} = 1$ are given for both simply supported and clamped panels. The results for simply supported panels indicate a smooth variation of $\left(\frac{\beta E}{q}\right)^{1/3} \frac{h}{a}$ with a/b; for the assumed stress condition $\left(\frac{N_y}{N_x} = 1\right)$ a simply supported panel always buckles in the first mode. For other values of N_y/N_x, however, critical values of a/b (at which the thickness required to prevent flutter becomes very large) could occur for simply supported panels (see ref. 5). For certain values of a/b $\left(\text{for example, } \frac{a}{b} = 1\right)$ the simply supported panels require greater thicknesses to prevent flutter than the clamped

panels. This result agrees with theoretical trends obtained for panels with no midplane stress (see, for example, refs. 18 and 20). However, in contrast to trends for unstressed panels, for values of a/b greater than about 1.4, the thicknesses required for simply supported panels are considerably smaller than those required for clamped panel. Thus, if buckling can occur, the assumption that a panel is simply supported is not necessarily a conservative assumption for flutter analyses. For practical panels the edge restraint will generally be somewhere between simply supported and clamped. The theoretical value of the thickness required to prevent flutter of such a panel could possibly be larger than the thicknesses obtained from analyses of either simply supported or clamped panels, depending on the buckling characteristics of the panel under consideration.

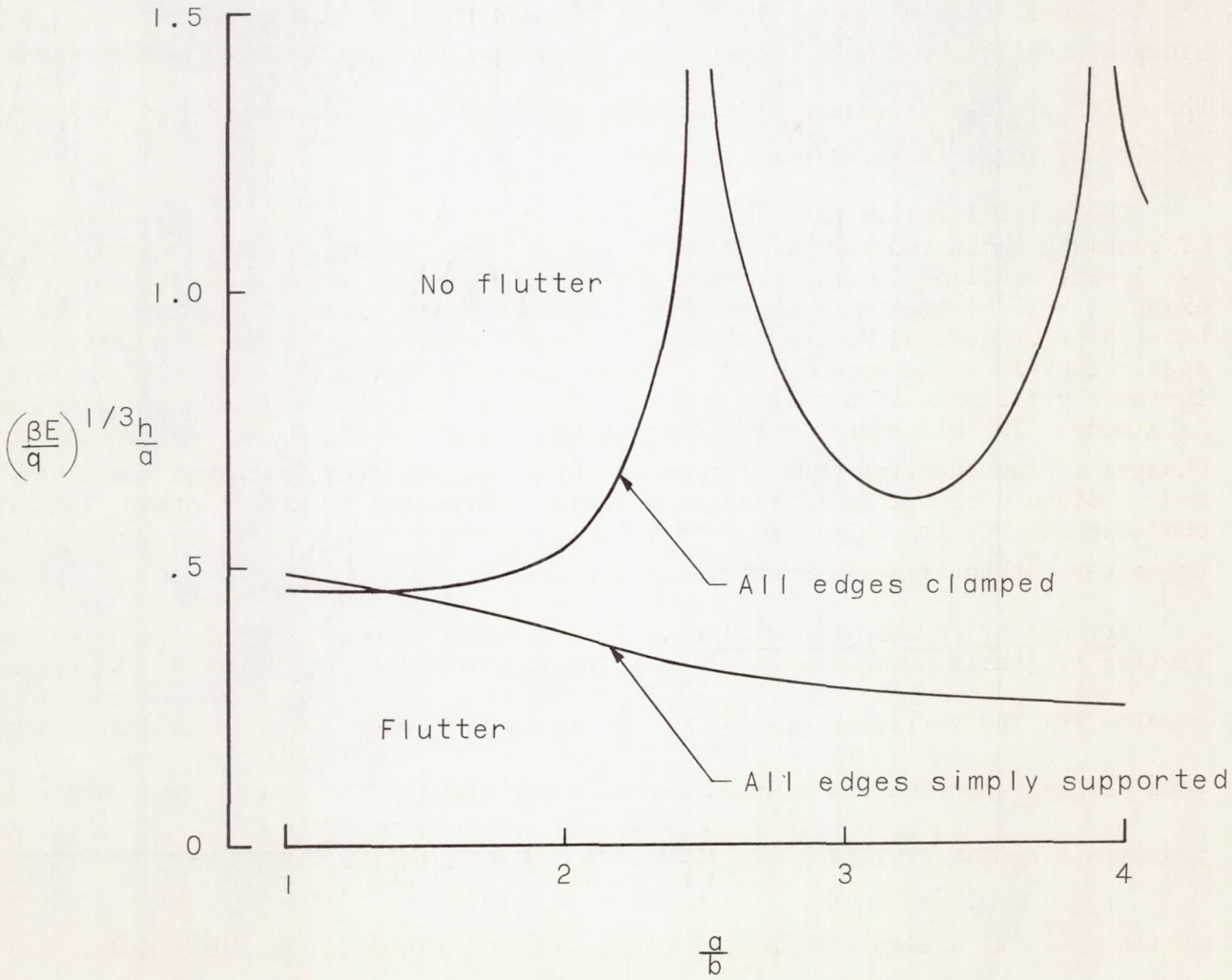

Figure 7.- Effects of boundary conditions on flutter characteristics of panels on the verge of buckling. $\frac{N_y}{N_x} = 1.0$.

Comparison of two-term and four-term flutter results.- Numerical results for flutter of clamped panels on the verge of buckling were obtained from two-term Galerkin solutions for comparison with the four-term results. The expansion functions used in the two-term analysis for a given value of a/b were such that the no-flow buckling loads corresponded to the two lowest buckling loads. The appropriate determinants are contained in equation (10). The results so obtained are compared with the four-term results in figure 8, which shows the variation of $\left(\frac{\beta E}{q}\right)^{1/3} \frac{h}{a}$ with a/b for $\frac{N_y}{N_x} = 1.0$. The trends obtained from the two-term

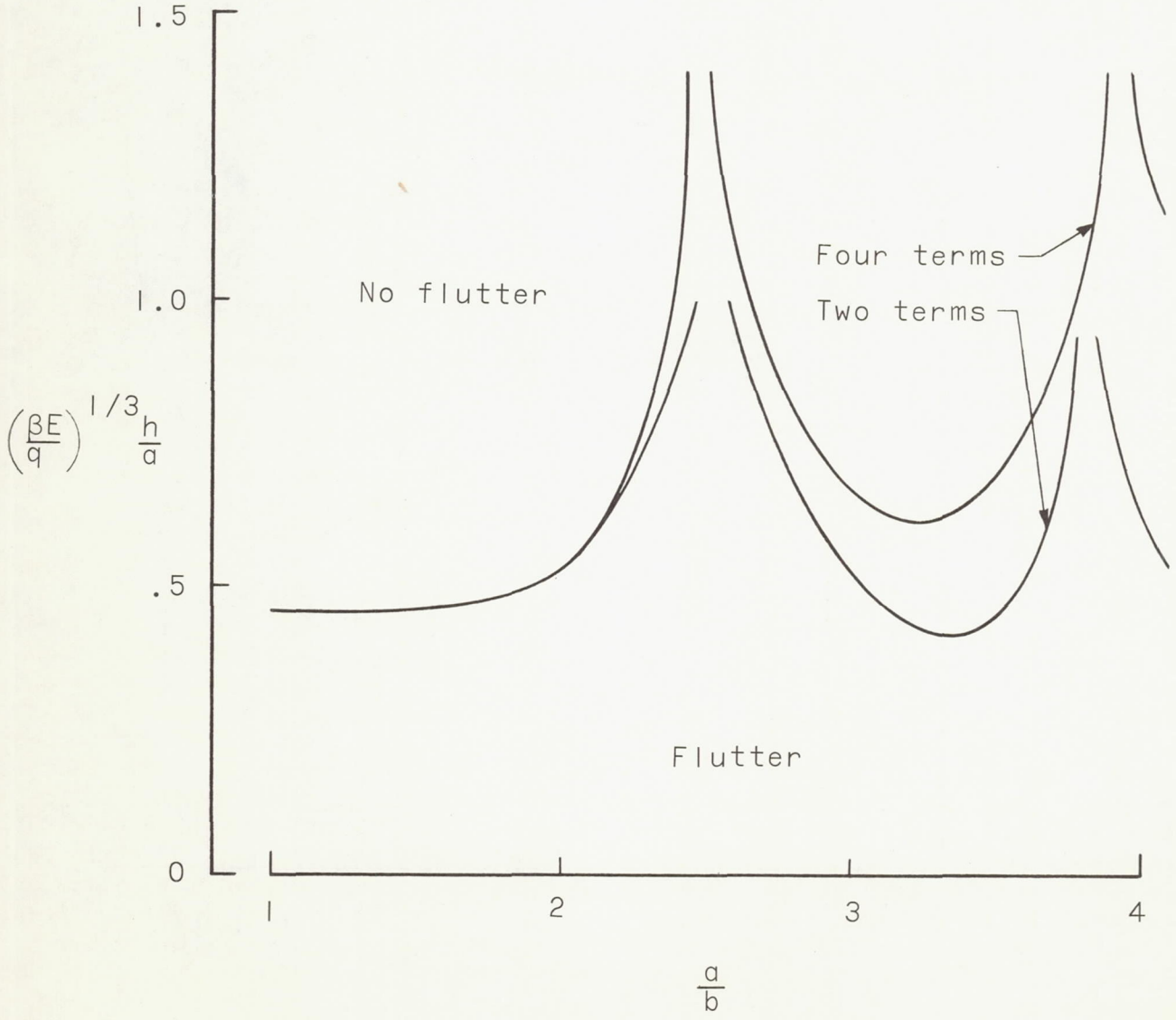

Figure 8.- Comparison of results obtained from two-term and four-term solutions for flutter. All edges clamped; $\frac{N_y}{N_x} = 1.0$.

solutions are in excellent agreement with the four-term results. However, for $\frac{a}{b} > 2.0$ the numerical agreement becomes poor in certain regions; this same trend is indicated in figure 3 in terms of the variation of $\bar{B}_c$ with $\bar{A}_c$. Better agreement between two-term and four-term results would be expected for simply supported panels since the expansion functions used in the analysis are the exact vibration (or buckling) modes for no airflow. In any event, it is apparent from the results presented in figure 8 that the accuracy of analytical predictions of the flutter characteristics of panels on the verge of buckling is strongly dependent on the validity of the analytical predictions of the panel buckling characteristics for no airflow.

EXPERIMENT

Tests

Panels.- The single-bay panels consisted of flat sheets of 0.040-, 0.063-, 0.081-, and 0.125-inch-thick 2024-T3 aluminum-alloy sheets attached to 0.375-inch-thick aluminum-alloy mounting plates by single rows of rivets along all four sides. The panel length and width (between center lines of rivet rows) were 25 inches and 6.25 inches, respectively. The panels were flush with the exposed surface of the mounting plates. The panel edge restraint approximated a fully clamped condition on all edges. Pertinent details of the panel construction are given in figure 9.

Tunnel.- All tests were conducted in the Langley 9- by 6-foot thermal structures tunnel, a Mach 3 intermittent blowdown facility exhausting to the atmosphere. A heat exchanger is preheated to provide stagnation temperatures up to 660° F and the stagnation pressure can be varied from 60 to 200 psia. Additional details regarding the tunnel may be found in reference 6.

Panel holder and mounting arrangement.- The panels were mounted in a panel holder which extended vertically through the test section (fig. 10). The panel holder has a half-wedge leading edge, flat sides, and a recess 29 inches wide, 30 inches high, and approximately 3.5 inches deep for accommodating test specimens. The recess is located on the nonbeveled side of the panel holder. Pneumatically operated sliding doors protect test specimens from aerodynamic buffeting and heating during tunnel starting and shutdown. Shock waves emanating from the doors are prevented from interfering with the airflow over the test specimen by means of aerodynamic fences. The flow conditions over the area of the recess are essentially free-stream conditions as determined from pressure surveys of a flat calibration panel (ref. 6). A vent-door arrangement on the side opposite the recess for the panel is used to control the pressure inside the cavity behind the test specimen.

All panels were mounted flush with the flat surface of the panel holder (see figs. 10 and 11). The mounting plate was attached to a mounting fixture which was bolted to the panel holder (fig. 11). Filler plates were mounted on either side of the test panel (see fig. 10) in order to cover the recess completely.

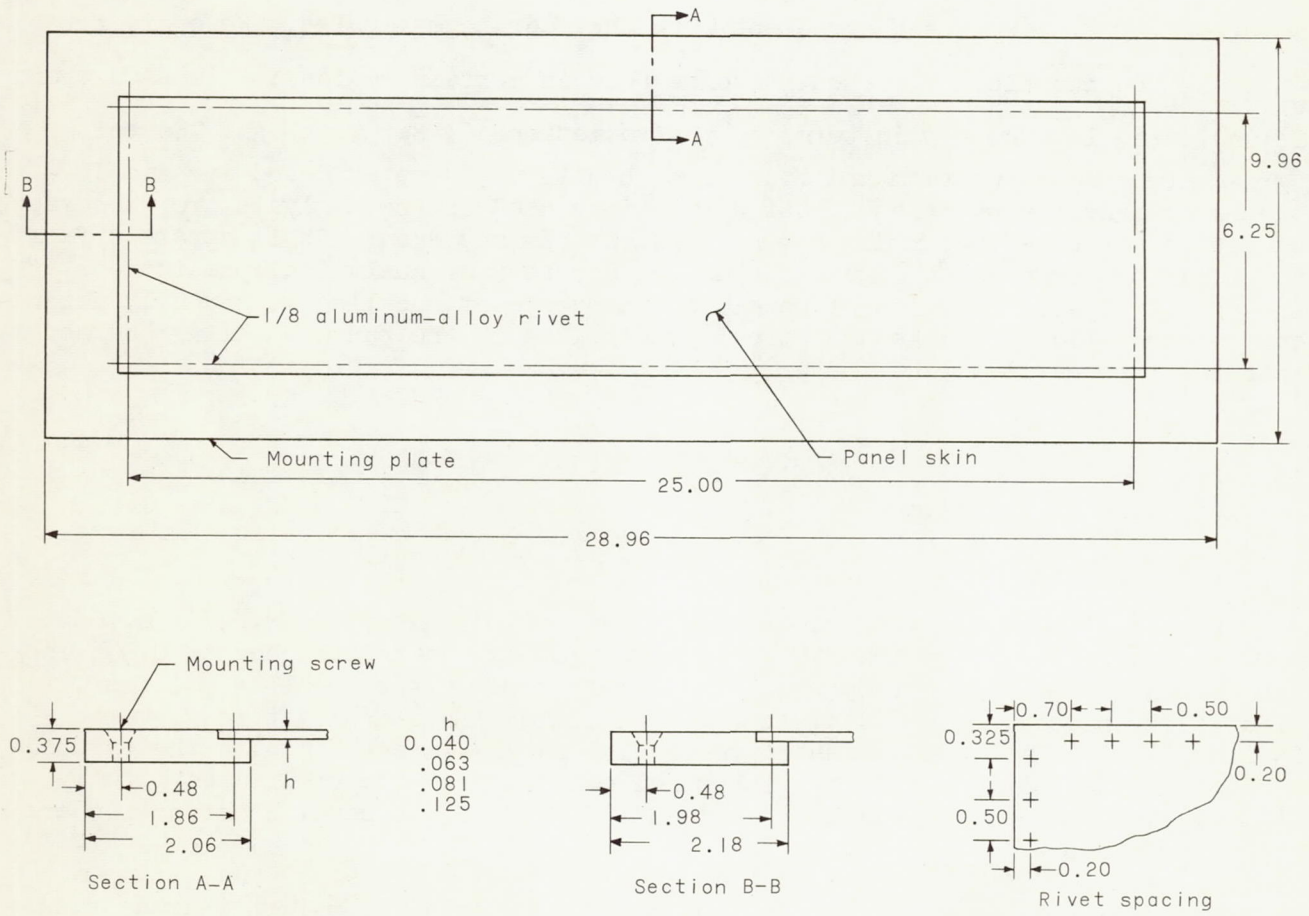

Figure 9.- Panel construction details (typical for all panels). All dimensions are in inches.

Instrumentation.- Iron-constantan thermocouples, spotwelded to the panels at the 7 locations shown in figure 12, were used to measure panel temperatures. Variable-reluctance deflectometers were used to determine the motion of the panel skin. The deflectometers were located approximately 1/4 inch behind the panel skin at the four positions indicated in figure 12. In addition, high-speed 16-mm motion pictures provided supplementary data on panel behavior. Grid lines were painted on the panel skins for photographic purposes.

Quick-response, strain-gage-type pressure transducers were used to measure static pressures at various locations on the panel holder and to measure the differential pressure acting on the panels. Tunnel stagnation pressures were obtained from static pressures measured in the settling chamber. Stagnation temperatures were measured by total-temperature probes located in the test section. For each test, all temperature and pressure data were recorded on magnetic tape. Deflectometer data and the differential pressures acting on the panels were recorded on high-speed oscillographs.

Test procedure.- The tests were conducted at a Mach number of 3.0, at dynamic pressures from 1,600 to 5,000 lb/sq ft, and at stagnation temperatures from 300°

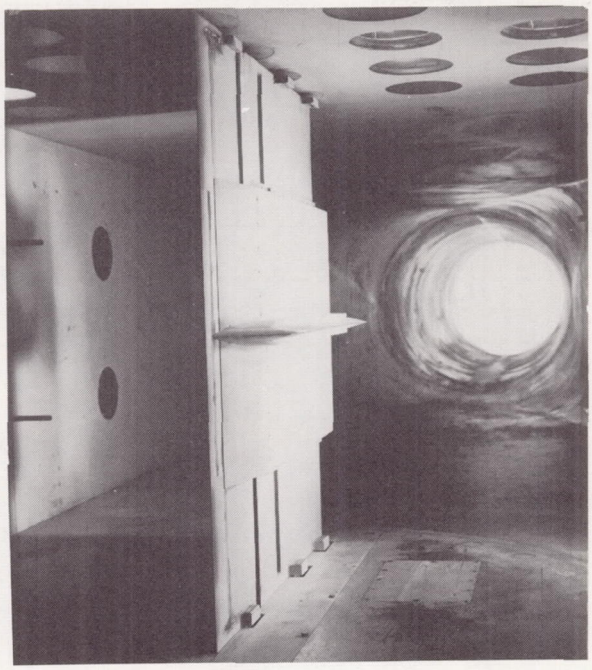

(a) Protective doors closed. L-60-5792

(b) Protective doors open. L-62-603

Figure 10.- Panel holder in test section as viewed from upstream.

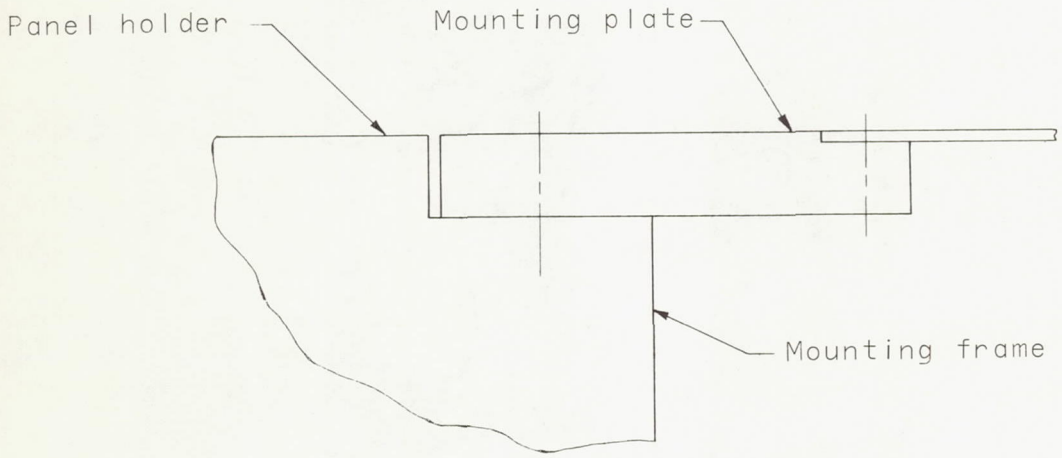

(a) Leading and trailing edges.

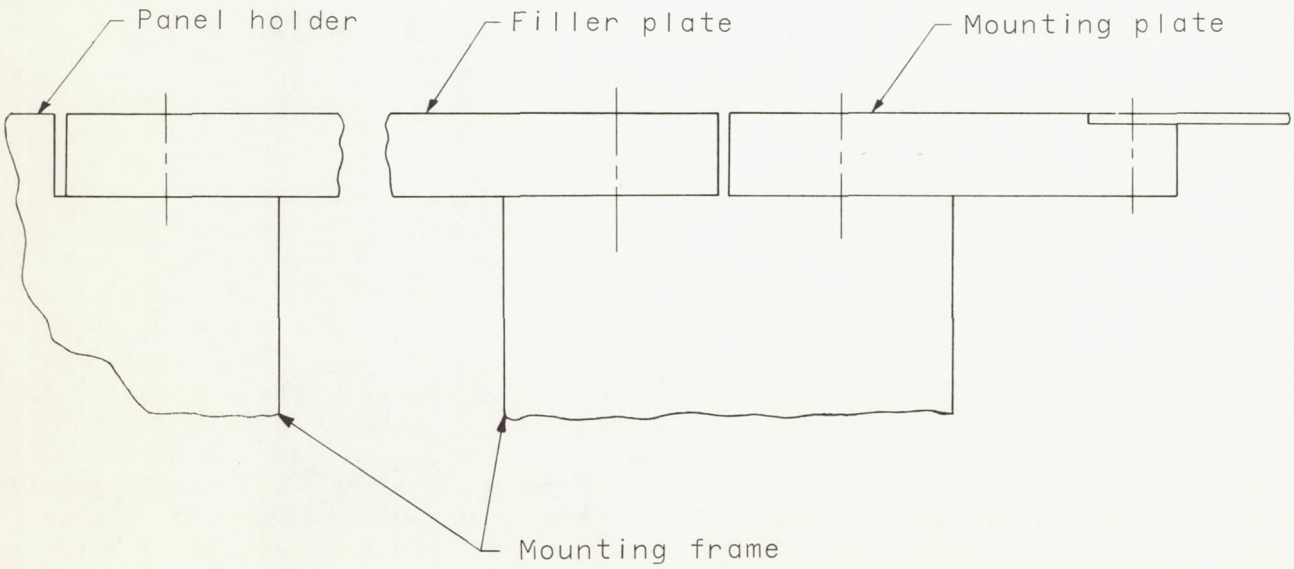

(b) Longitudinal edges.

Figure 11.- Panel mounting arrangement (typical for all panels).

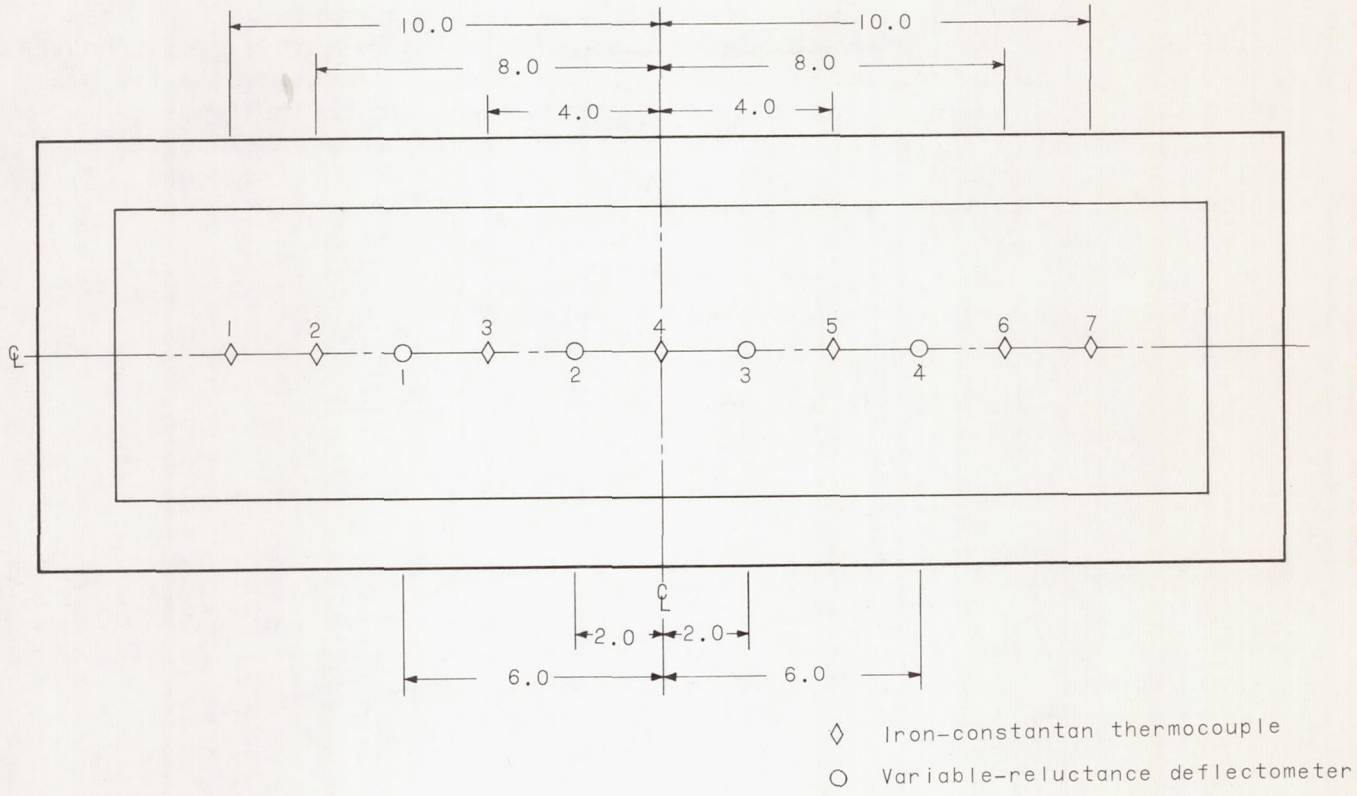

Figure 12.- Location of panel instrumentation (all dimensions are in inches).

to 650° F. The protective doors on the panel holder were opened after desired test conditions were established. The dynamic pressure was held constant during the first few seconds of all tests, but was varied during the remainder of some tests in an attempt to obtain additional flutter points. The occurrence of flutter was determined by monitoring the high-speed oscillographs during a test.

The usual procedure for varying the dynamic pressure was as follows: (a) If flutter had started and stopped, the dynamic pressure was increased in an attempt to restart flutter; (b) if the panel was fluttering near the end of a test, the dynamic pressure was decreased in an attempt to stop flutter. The differential pressure acting on the panels was controlled manually in an attempt to keep the differential pressure as small as possible; in some tests malfunction of the monitoring instrumentation prevented accurate control of Δp. The stagnation temperature was essentially constant during most tests but decreased during the latter portion of several tests. The protective doors were closed 3 seconds prior to tunnel shutdown. The duration of test conditions varied between 10 and 60 seconds.

Results and Discussion

In seven of the eight tests made in this investigation, flutter was induced in panels that were flat prior to the start of flutter. The flutter stopped in

three of these tests; at the cessation of flutter the panels were in a buckled condition. In one test, after flutter had stopped it was restarted by increasing the dynamic pressure. No flutter occurred in one test. Pertinent data for all tests are given in table I. The data tabulated are the stagnation temperature T_t, dynamic pressure q, panel differential pressure Δp, average center-line temperature T of the panel skin, average skin-temperature increase ΔT, and frequency f at the start of flutter.

TABLE I.- PANEL FLUTTER DATA

$$\left[E = 10.5 \times 10^6 \text{ psi}; \alpha = 12.6 \times 10^{-6} \frac{\text{in./in.}}{^\circ F}\right]$$

Test	h, in.	T_t, °F	Flutter start					Flutter stop				No flutter			
			q, psf	Δp, psi	T, °F	ΔT, °F	f, cps	q, psf	Δp, psi	T, °F	ΔT, °F	q, psf	Δp, psi	T, °F	ΔT, °F
1	0.040	310	2,260	-0.19	73	7	170	1,855	-0.16	165	99				
			[a]1,860	-.33	174	108	110								
2	.063	310	5,030	-.26	77	17	300	4,940	-.37	181	121				
3	.063	300	3,470	-.08	114	48	300								
4	.063	315	2,490	-.10	112	48	290								
5	.081	305	4,470	-.04	113	39	350								
6	.081	400	1,640	-.04	150	77	260								
7	.125	650	4,940	-.06	242	160	440	4,940	-.05	285	204				
8	.125	500										4,200	-0.06	253	181

[a]Panel buckled prior to the start of flutter.

Panel temperatures.- During the first 3 seconds of every test the panels were protected from aerodynamic heating by the protective doors, and any temperature increase of the panel skin during this time was usually insignificant. After the panels were exposed to the airstream, the skin temperature increased in a manner similar to the typical temperature histories shown in figure 13 (test 7). The top curve represents the average skin temperature for thermocouples 2 to 6. The lower curve represents the average of thermocouples 1 and 7 (which were nearest the leading edge and trailing edge, respectively). The difference in the curves suggests that there was some conduction along the longitudinal center line of the panel near the leading and trailing edges; similar conduction effects could be expected near the longitudinal edges. However, these temperature variations were neglected in analyzing the test data, and the average increase in temperature for thermocouples 1 to 7 was considered to be the average temperature increase ΔT of the panel.

Flutter parameters.- The flutter data obtained in this investigation are summarized in terms of a dimensionless flutter parameter and a dimensionless modified

temperature parameter. Of the quantities in the flutter parameter $\left(\frac{q}{\beta E}\right)^{1/3}\frac{a}{h}$, only the dynamic pressure q and skin thickness h were varied in this investigation. Because of the short duration of the tests and the relatively low panel temperatures, changes in material properties with temperature were assumed to be negligible.

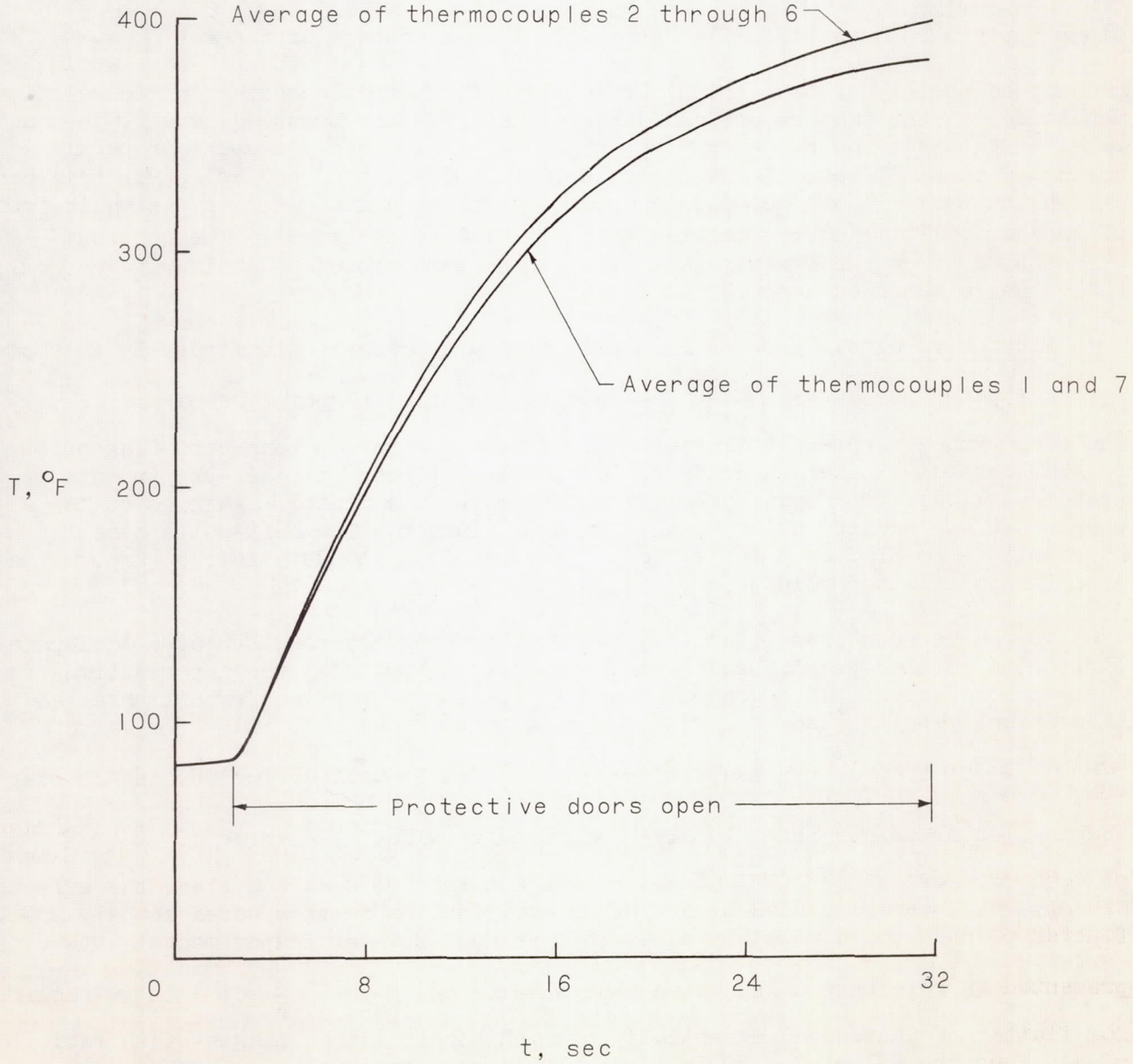

Figure 13.- Measured skin temperatures of panel for test 7.

The effects of midplane stress and buckling are indicated, in terms of the skin-temperature rise ΔT and the differential pressure Δp, by the modified temperature parameter ψ:

$$\psi = \pm \frac{12(1 + \mu)}{\pi^2} \left\{ \pm \alpha \Delta T \left(\frac{a}{h}\right)^2 - C \left[\frac{\Delta p}{E} \left(\frac{a}{b}\right)^4 \right]^{2/3} \right\} \tag{13}$$

In the expression for ψ, which was first used in reference 21, the positive signs apply when a panel is flat as ψ is then a measure of the ratio $\frac{N_x}{\pi^2 D/a^2}$ and may be positive (compression) or negative (tension) depending on the relative magnitudes of the temperature and differential pressure terms. However, when a panel is buckled, the negative signs apply as ψ is then a measure of buckle depth and both ΔT and Δp tend to increase the depth of buckle. (For this condition the panel is subjected to compressive stress and the negative sign in front of the term $12(1 + \mu)/\pi^2$ insures that ψ will be positive.) The constant C was obtained from the experimental data by the same procedure as in reference 21; the value so obtained was 0.25.

Flutter results.- Results from all tests are presented in figure 14 in terms of the flutter parameter $\left(\frac{q}{\beta E}\right)^{1/3} \frac{a}{h}$ and the modified temperature parameter ψ. The open symbols represent flutter-start points for panels that were flat prior to the start of flutter, and the solid symbols represent flutter-stop points (panel buckled). The open symbol with tick mark is a flutter-start point for a panel that was buckled prior to the start of flutter. The half-solid symbol represents a no-flutter point. The solid curve is a boundary faired through the experimental flutter points.

As can be seen from figure 14, the flutter boundary consists of a flat-panel portion, a buckled-panel portion, and a transition point at the intersection of the two boundaries. This general trend is similar to previous experimental and theoretical results (see, for example, refs. 6 to 8 and ref. 10). The value of $\left(\frac{q}{\beta E}\right)^{1/3} \frac{a}{h}$ of 1.90 at the transition point is fairly well defined by the flutter and no-flutter points that closely bracket this value. The value of $\left(\frac{q}{\beta E}\right)^{1/3} \frac{a}{h}$ of 4.50 for zero stress ($\psi = 0$) may be subject to some question since the effects of Δp, which were included by use of an empirical expression based on only a few flutter points, could possibly alter this value. However, experimental data presented in reference 8 indicated that a value of $\left(\frac{q}{\beta E}\right)^{1/3} \frac{a}{h}$ of 4.35 is required for flutter of unstressed essentially clamped panels with a length-width ratio of 4. Thus the value of 4.50 in figure 14 appears reasonable. The results shown in figure 14 indicate that the thickness required to prevent flutter at the transition point is more than twice the thickness required to prevent flutter for $\psi = 0$.

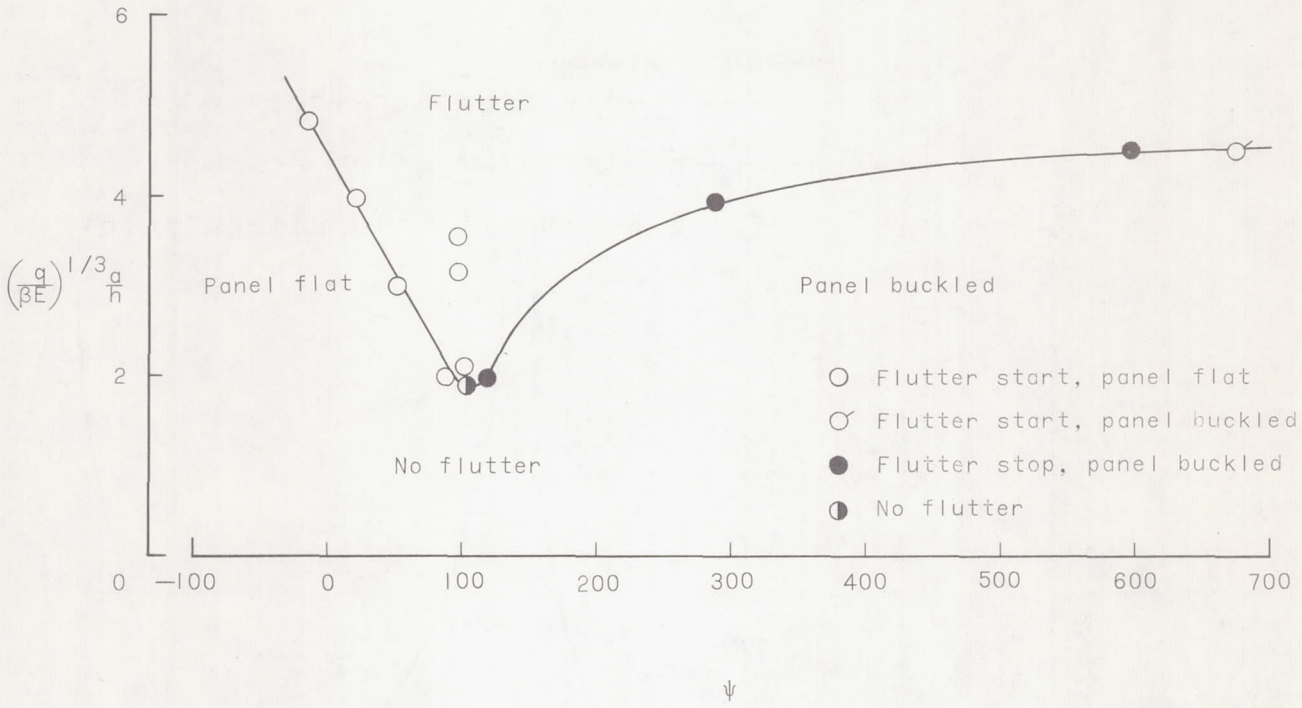

Figure 14.- Effects of thermal stress and buckling on flutter of clamped panels with length-width ratio of 4.

High-speed motion pictures revealed that all observed flutter appeared to be of the sinusoidal traveling-wave type. The flutter mode appeared to have three half-waves in the direction of airflow and was similar to the buckling mode; the similarity of flutter and buckling modes has been observed previously (see, for example, ref. 6). The calculated no-flow buckling mode also had three half-waves in the longitudinal direction (direction of airflow). Thus the experimental results of this investigation tend to verify the conjecture made earlier that a reasonable estimate of the number of half-waves in the flutter mode of a stressed panel could be obtained by determining the panel's buckling mode.

COMPARISON OF THEORY AND EXPERIMENT

The flutter envelopes presented in references 3 and 4 are reproduced in figure 15 in terms of the flutter parameter $\left(\frac{\beta E}{q}\right)^{1/3}\frac{h}{a}$ and a/b. The original envelope (ref. 3) represents an empirical flutter boundary faired through maximum values of the flutter parameter for all experimental panel flutter data available at that time. The flutter envelope presented in reference 4 is a revision of the original envelope based on experimental data obtained since publication of reference 3. As can be seen from figure 15, the flutter envelopes indicate that $\left(\frac{\beta E}{q}\right)^{1/3}\frac{h}{a}$ decreases as a/b increases. Also shown in figure 15 is the variation

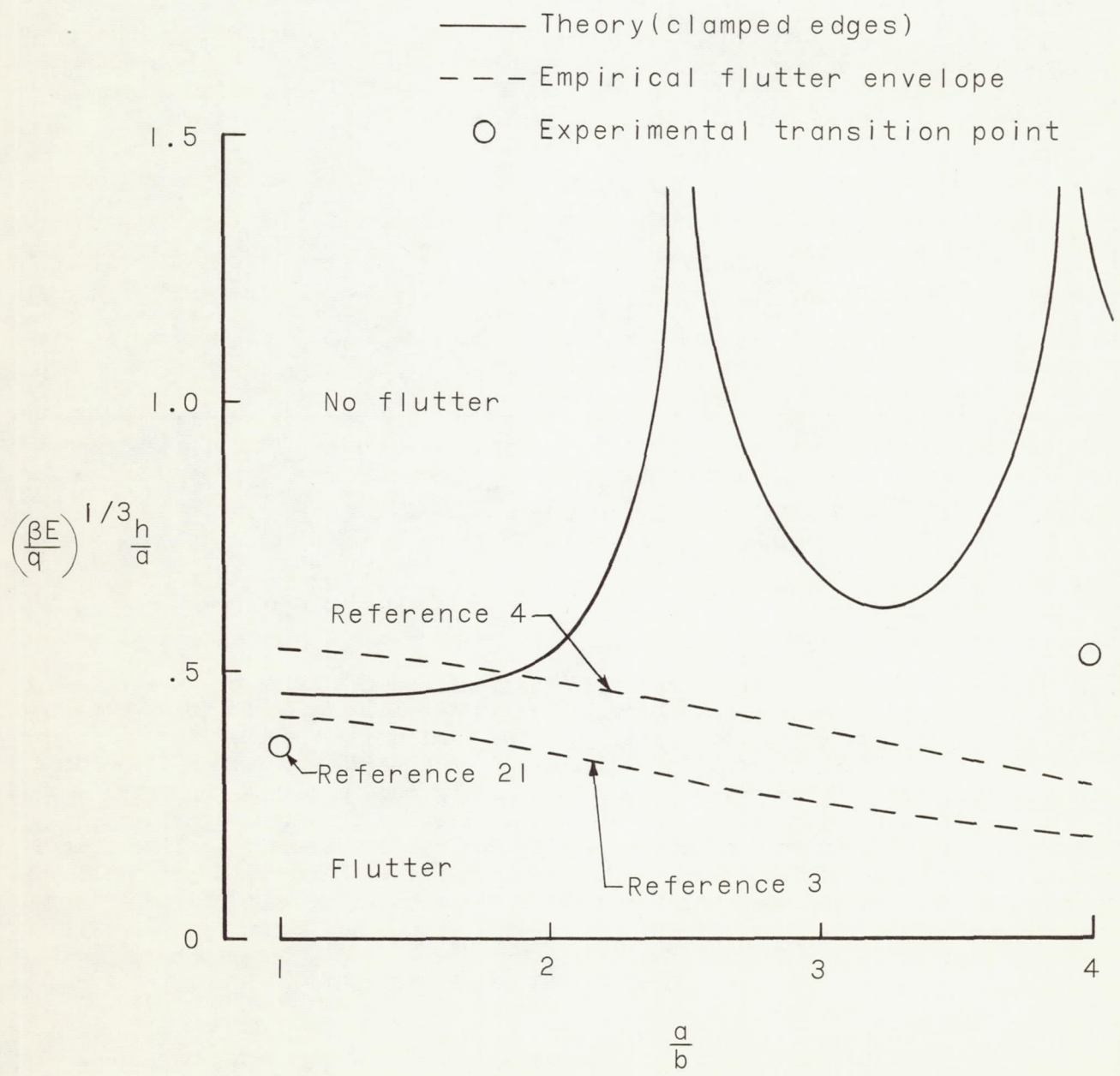

Figure 15.- Comparison between theory and experiment for flutter of panels on the verge of buckling. All edges clamped; $\frac{N_y}{N_x} = 1.0$.

of $\left(\frac{\beta E}{q}\right)^{1/3}\frac{h}{a}$ with a/b for $\frac{N_y}{N_x} = 1$ and all edges clamped, as obtained from the four-term analysis presented herein. Experimentally determined transition points obtained for essentially clamped panels with a/b of 0.96 (ref. 21) and 4 (present investigation) are indicated in figure 15 by the symbols; the stress ratio N_y/N_x for these panels was approximately 1.0.

The experimental point for $\frac{a}{b} = 0.96$ falls within the flutter region as indicated by theory and both flutter envelopes. Thus, for this case both theory and the flutter envelopes are adequate as design criteria for preventing flutter. However, the experimental point for $\frac{a}{b} = 4$ falls within the flutter region indicated by theory but well within the no-flutter region as defined by both flutter envelopes. Thus, for this case both experimental flutter envelopes were inadequate as design criteria. Indeed, the theoretical results presented herein suggest that the flutter envelope could be inadequate for predicting flutter of stressed panels over a wide range of a/b for many combinations of edge restraint and stress ratio, particularly if buckling could occur. However, the flutter envelopes might be useful for predicting flutter of unstressed panels.

For $\frac{a}{b} = 0.96$ the theoretical value of $\left(\frac{\beta E}{q}\right)^{1/3}\frac{h}{a}$ of 0.455 is 27 percent greater than the experimental value (0.357). For $\frac{a}{b} = 4.0$ the numerical agreement is poor. However, several factors could affect the agreement at this point. As can be seen from figures 5 and 6, slight changes in a/b or N_y/N_x (both of which are not known exactly) could cause considerable change in the value of the flutter parameter $\left(\frac{\beta E}{q}\right)^{1/3}\frac{h}{a}$. In addition, the differential pressure loading, which was present in the experiments, was neglected in the analysis. Moreover, the experimental data point for a/b of 4 is in the vicinity of a portion of the theoretical flutter boundary where nonlinear effects, which were neglected in the analysis, could be significant. In any event, the results shown in figure 15 indicate that small-deflection transtability analyses appear to give conservative results.

CONCLUSIONS

The flutter characteristics of finite panels on the verge of buckling have been examined both theoretically and experimentally. The governing differential equation for small deflections was solved by the Galerkin method. Transtability flutter boundaries were obtained from four-term solutions for both simply supported and clamped panels with various length-width ratios and various ratios of lateral to longitudinal midplane compressive stress. In addition, essentially clamped aluminum-alloy panels with a length-width ratio of 4 were tested in the Langley 9- by 6-foot thermal structures tunnel in order to obtain experimental

data on the effects of thermally induced midplane compressive stress and buckling on panel flutter. The tests were conducted at a Mach number of 3.0 at dynamic pressures ranging from 1,600 to 5,000 lb/sq ft and at stagnation temperatures from 300° to 650° F. The theoretical and experimental results revealed the following:

1. The theoretical (transtability) flutter characteristics of panels are very sensitive to the buckling characteristics of the panels.

2. For given panel boundary conditions, there are many critical combinations of length-width ratio and ratio of lateral to longitudinal midplane compressive stress for which theory indicates that the thickness required to prevent flutter becomes very large. These critical combinations result when the panel has an equal choice of two modes for buckling with no airflow.

3. The panel buckling characteristics apparently dictate the flutter mode at the transition point.

4. The assumption of simply supported edges is not necessarily a conservative assumption for flutter analyses if buckling can occur.

5. The test data revealed an overall flutter boundary that consisted of a flat-panel portion, a buckled-panel portion, and a transition point at the intersection of the two. At the transition point the thickness required to prevent flutter was more than twice the thickness required to prevent flutter of an unheated (unstressed) panel.

6. The experimental results for flutter of panels on the verge of buckling were within the envelope provided by the small-deflection transtability calculations. Both theory and experiment indicated that existing empirical panel flutter envelopes may be inadequate as flutter criteria for stressed panels.

Langley Research Center,
National Aeronautics and Space Administration,
Langley Station, Hampton, Va., June 17, 1963.

REFERENCES

1. Kordes, Eldon E., and Noll, Richard B.: Flight Flutter Results for Flat Rectangular Panels. NASA TN D-1058, 1962.

2. Fung, Y. C. B.: A Summary of the Theories and Experiments on Panel Flutter. AFOSR TN 60-224, Guggenheim Aero. Lab., C.I.T., May 1960.

3. Kordes, Eldon E., Tuovila, Weimer J., and Guy, Lawrence D.: Flutter Research on Skin Panels. NASA TN D-451, 1960.

4. Hess, Robert W., and Gibson, Frederick W.: Experimental Investigation of the Effects of Compressive Stress on the Flutter of a Curved Panel and a Flat Panel at Supersonic Mach Numbers. NASA TN D-1386, 1962.

5. Guy, Lawrence D., and Dixon, Sidney C.: A Critical Review of Experiment and Theory for Flutter of Aerodynamically Heated Panels. Symposium on Dynamics of Manned Lifting Planetary Entry, S. M. Scala, A. C. Harrison, and M. Rogers, eds., John Wiley & Sons, Inc., c.1963, pp. 568-595.

6. Dixon, Sidney C., Griffith, George E., and Bohon, Herman L.: Experimental Investigation at Mach Number 3.0 of the Effects of Thermal Stress and Buckling on the Flutter of Four-Bay Aluminum Alloy Panels With Length-Width Ratios of 10. NASA TN D-921, 1961.

7. Guy, Lawrence D., and Bohon, Herman L.: Flutter of Aerodynamically Heated Aluminum-Alloy and Stainless-Steel Panels With Length-Width Ratio of 10 at Mach Number of 3.0. NASA TN D-1353, 1962.

8. Bohon, Herman L.: Panel Flutter Tests on Full-Scale X-15 Lower Vertical Stabilizer at Mach Number of 3.0. NASA TN D-1385, 1962.

9. Isaacs, R. P.: Transtability Flutter of Supersonic Aircraft Panels. U.S. Air Force Project RAND P-101, The RAND Corp., July 1, 1949.

10. Fralich, Robert W.: Postbuckling Effects on the Flutter of Simply Supported Rectangular Panels at Supersonic Speeds. NASA TN D-1615, 1963.

11. Leonard, Robert W., and Hedgepeth, John M.: Status of Flutter of Flat and Curved Panels. NACA RM L57D24c, 1957.

12. Hayes, W.: A Buckled Plate in a Supersonic Stream. Rep. No. AL-1029, North American Aviation, Inc., May 10, 1950.

13. Miles, John W.: Dynamic Chordwise Stability at Supersonic Speeds. Rep. No. AL-1140, North American Aviation, Inc., Oct. 18, 1950.

14. Hedgepeth, John M.: Flutter of Rectangular Simply Supported Panels at High Supersonic Speeds. Jour. Aero. Sci., vol. 24, no. 8, Aug. 1957, pp. 563-573, 586.

15. Sokolnikoff, I. S.: Mathematical Theory of Elasticity. Second ed., McGraw-Hill Book Co., Inc., 1956, pp. 421-425.

16. Young, Dana, and Felgar, Robert P., Jr.: Tables of Characteristic Functions Representing Normal Modes of Vibration of a Beam. Pub. No. 4913, Eng. Res. Ser. No. 44, Bur. Eng. Res., Univ. of Texas, July 1, 1949.

17. Felgar, Robert P., Jr.: Formulas for Integrals Containing Characteristic Functions of a Vibrating Beam. Cir. No. 14, Bur. Eng. Res., Univ. of Texas, 1950.

18. Houbolt, John C.: A Study of Several Aerothermoelastic Problems of Aircraft Structures in High-Speed Flight. Nr. 5, Mitteilungen aus dem Institut für Flugzeugstatik und Leichtbau. Leemann (Zürich), c.1958.

19. Libove, Charles, and Stein, Manuel: Charts for Critical Combinations of Longitudinal and Transverse Direct Stress for Flat Rectangular Plates. NACA WR L-224, 1946. (Formerly NACA ARR L6A05.)

20. Nelson, Herbert C., and Cunningham, Herbert J.: Theoretical Investigation of Flutter of Two-Dimensional Flat Panels With One Surface Exposed to Supersonic Potential Flow. NACA Rep. 1280, 1956. (Supersedes NACA TN 3465.)

21. Dixon, Sidney C.: Experimental Investigation at Mach Number 3.0 of Effects of Thermal Stress and Buckling on Flutter Characteristics of Flat Single-Bay Panels of Length-Width Ratio 0.96. NASA TN D-1485, 1962.